The Structure of the Nonadiabatic Photochemical *Trans* → *Cis* Isomerization Channel in *All-Trans* Octatetraene

Marco Garavelli,† Paolo Celani, Naoko Yamamoto,‡ Fernando Bernardi,† Michael A. Robb,*,‡ and Massimo Olivucci*,†

Dipartimento di Chimica "G.Ciamician" dell' Università di Bologna, Via Selmi 2 40126 Bologna, Italy
King's College London London WC2R 2LS, United Kingdom

Received May 20, 1996
Revised Manuscript Received August 26, 1996

The photoinduced double-bond *trans* → *cis* isomerization of polyenes provides a model for understanding many processes of basic importance in photochemistry[1a] and photobiology.[1b] Recent spectroscopic low-temperature investigations of isolated polyene molecules are providing evidence that this process may occur *nonadiabatically*. Christensen et al.[2] have proposed that (under isolated conditions in a cool jet) *trans* → *cis* motion in *all-trans*-octa-1,3,5,7-tetraene (*all-trans*-OT) induces the opening of an efficient nonadiabatic radiationless deactivation channel on S_1 (2Ag).

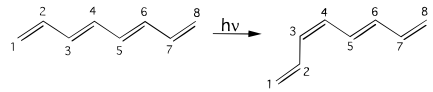

(1)

In contrast, matrix isolation studies by Kohler,[3] indicate that the photoisomerization on the S_1 state occurs *adiabatically* (i.e., prior to decay to the ground state S_0) by overcoming a ∼870 cm^{-1} (2.5 kcal mol^{-1}) barrier. This adiabatic reaction is activated ∼150 K below the temperature required for efficient radiationless deactivation.[3]

In this paper we use MCSCF[4] and multireference MP2[5] methods to document the low-lying transition states and minimum energy paths (MEP) of an isolated S_1 *all-trans*-OT molecule.[6] A schematic representation of the computed S_1/S_0 potential surface is shown in Figure 1. In the jet experiments of Christensen et al., the opening of the radiationless deactivation channel is monitored by gradually increasing the S_1 excess vibrational energy, and these low-energy conditions are modeled by our MEP computations (arrows in Figure 1). The process which is seen in the jet experiment is shown to correspond to initial *trans* → *cis* isomerization motion leading (via the transition state $TS_{E\rightarrow Z(nonadiab)}$ in Figure 1) to a point where the

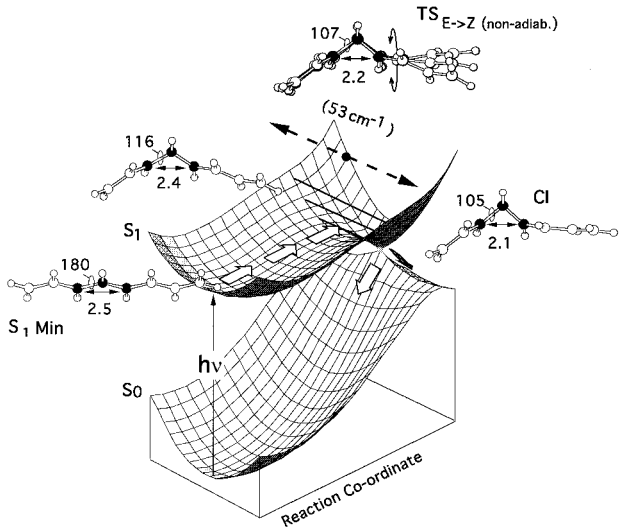

Figure 1. Two-dimensional overwiev of the S_1 and S_0 potential energy surfaces of *all-trans*-OT. The arrows illustrate the S_1 MEP through the saddle point region corresponding to $TS_{E\rightarrow Z(nonadiab)}$. (The computed S_1 and S_0 energy profiles along the S_1 MEP are given in Figure 3 of supporting information.) The structures (relevant parameters in angstroms and degrees) illustrate the geometrical progression along the MEP. The position of the $-(CH)_3-$ kink is marked by three filled carbon atoms. The motion (dashed double arrow) corresponding to the lowest frequency (53 cm^{-1}) vibrational mode orthogonal to the isomerization direction is illustrated via three superimposed structures at the transition state point.

S_1 and S_0 energy surfaces are *conically* intersecting (CI in Figure 1) and fully efficient radiationless decay is possible. Our computations suggest that the nonadiabatic isomerization hypothesis of Christensen et al. is correct because our computed S_1 potential surface is consistent with the following experimental facts:[2] (i) The decay rate undergoes an abrupt increase for excess energies >2100 cm^{-1} (∼6.0 kcal mol^{-1}) and (ii) the rate increase occurs in a stepwise fashion with a ∼80 cm^{-1} long initial step.[7] (The steps in the rate data reflect the quantization of the vibrational motion orthogonal to the transition vector.[8] In particular, the length of the initial step is a measure of the energy separation between the zero-point energy and the *first* real excited vibrational level of the transition structure.)

We have located four competitive reactive channels starting from the S_1 *all-trans*-OT equilibrium structure (S_1 Min, Figure 2a). The energies and geometries of the TS that define these channels are collected in Table 1 and Figure 2b−e. The channel for nonadiabatic C_3-C_4 *trans* → *cis* double-bond isomerization ($TS_{E\rightarrow Z(nonadiab)}$, Figure 2b) is the lowest energy one. At higher energy, one has a nonadiabatic ($TS_{CH_2(nonadiab)}$, Figure 2c) and adiabatic ($TS_{CH_2\text{-}twist(adiab)}$, Figure 2d) C_1-C_2 double-bond rotation channel where the CH_2 group is ∼90° rotated. A fully

† Università di Bologna.
‡ King's College London.

(1) (a) Saltiel, J.; Sears, D. F., Jr.; Ko, D.-H.; Park, K.-M. In *CRC Handbook of Organic Photochemistry and Photobiology*; Horspool, W. M., Song, P.-S., Eds.; CRC Press: Boca Raton, FL, 1995; pp 3−15. (b) Liu, R. S. H. *Ibid*; pp 165−172.
(2) Petek, H.; Bell, A. J.; Young, S. C.; Taek-Soo, K.; Yoshihara, K.; Tounge, B. A.; Christensen, R. L. *J. Chem. Phys.* **1993**, *98*, 3777−3794.
(3) Kohler, B. E. *Chem. Rev.* **1993**, *93*, 41−54.
(4) The MCSCF program we used is implemented in *Gaussian 94*, Revision B.2. See: Frisch, M. J.; Trucks, G. W.; Schlegel, H. B.; Gill, P. M. W.; Johnson, B. G.; Robb, M. A.; Cheeseman, J. R.; Keith, T.; Petersson, G. A.; Montgomery, J. A.; Raghavachari, K.; Al-Laham, M. A.; Zakrzewski, V. G.; Ortiz, J. V.; Foresman, J. B.; Peng, C. Y.; Ayala, P. Y.; Chen, W.; Wong, M. W.; Andres, J. L.; Replogle, E. S.; Gomperts, R.; Martin, R. L.; Fox, D. J.; Binkley, J. S.; Defrees, D. J.; Baker, J.; Stewart, J. P.; Head-Gordon, M.; Gonzalez, C.; Pople, J. A. *Gaussian 94*, Revision B.2.; Gaussian, Inc.: Pittsburgh, PA, 1995.
(5) (a) Andersson, K.; Malmqvist, P.-A.; Ross, B. O. *J. Chem. Phys.* **1992**, *96*, 1218. (b) *MOLCAS*, Version 3; Andersson, K.; Blomberg, M. R. A.; Fülscher, M.; Kellö, V.; Lindh, R.; Malmqvist, P.-A.; Noga, J.; Olsen, J.; Roos, B. O.; Sadlej, A. J.; Siegbahn, P. E. M.; Urban, M.; Widmark, P. O. University of Lund, Sweden, 1994.

(6) All computations have been carried out using a complete active space (CAS) with the D95* (DZ+d) and/or the 6-31G* basis sets available in *Gaussian 94*.[4] The S_1 MEP and frequencies have been computed using an eight electrons in eight orbitals CAS and the 6-31G* basis set. The conical intersection structure CI has been determined as the last point of the computed MEP before MSCSF root flipping (see supporting information). In order to improve the energetics by including the effect of dynamic electron correlation, the MCSCF energies have been recomputed at the multireference Møller−Plesset perturbation theory method using the PT2F method[5a] included in *MOLCAS-3*.[5b] A similar procedure (MCSCF DZ+d and 6-31G* optimization + MRCI energy computations) has been recently used to succesfully reproduce the *all-trans*-OT 1Ag → 2Ag absorption spectra. See: Buma, W. J.; Zerbetto, F. *J. Chem. Phys.* **1995**, *103*, 10492.

(7) Young, S. C.; Taek-Soo, K.; Petek, H.; Yoshihara, K.; Christensen, R. L. *J. Chem. Phys.* **1994**, *100*, 9269−9271.
(8) (a) Chatfield, D. C.; Friedman, R. S.; Truhlar, D. G.; Garrett, B. C.; Schwenke, D. W. *J. Am. Chem. Soc.* **1991**, *113*, 486−494. (b) Marcus, R. A. *Science* **1992**, *256*, 1523.

S0002-7863(96)01707-6 CCC: $12.00

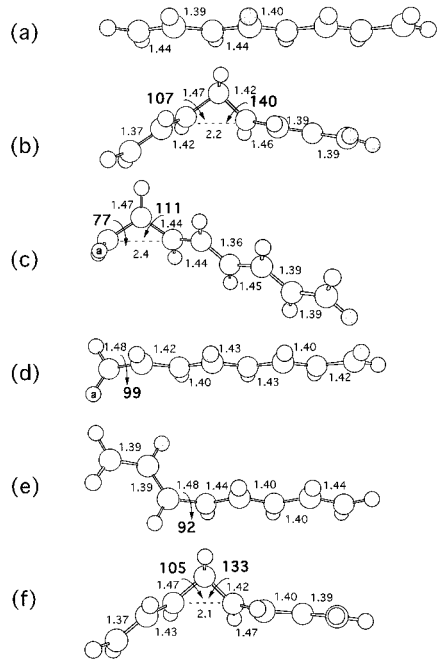

Figure 2. Structures corresponding to (a) the S_1 *all-trans*-OT structure (S_1 Min), (b) $TS_{E\rightarrow Z(\text{nonadiab})}$, (c) $TS_{CH_2(\text{nonadiab})}$, (d) $TS_{CH_2\text{-twist(adiab)}}$, (e) $TS_{E\rightarrow Z(\text{adiab})}$, and (f) the S_1/S_0 intersection structure (CI). The relevant geometrical parameters are given in angstroms and degrees ($H_a-C-C-C$ and $C-C-C-C$ torsions are in bold).

Table 1. Multireference−MP2 Absolute (*E*) and Relative (ΔE) Energies[6]

structure	state	E_{au} S_1[a]	w^b	ΔE (kcal mol^{-1})[a]	exp[c]
S_0 Min	S_0	−309.84471	0.76	−76.7	−82.3
		(−309.75183)	0.76	(−78.4)	
S_1 Min	S_1	−309.72241	0.75	0.0	0.0
		(−309.62694)	0.75	0.0	
$TS_{E\rightarrow Z(\text{nonadiab})}$	S_1	−309.71034	0.74	7.6	6.0
		(−309.61422)	0.75	(8.0) (7.4[d])	
$TS_{CH_2(\text{nonadiab})}$	S_1	−309.70645	0.75	10.0	
$TS_{CH_2\text{-twist(adiab)}}$	S_1	−309.70428	0.75	11.4	
$TS_{E\rightarrow Z(\text{adiab})}$	S_1	−309.69877	0.75	14.8	

[a] Values computed using the D95* and 6-31G* (values in parentheses) basis sets. [b] The weight of CAS−SCF reference function (i.e., the zeroth order function) in the first order function. [c] See ref 2. [d] Zero-point energy corrected value.

adiabatic C_3-C_4 *trans* → *cis* isomerization ($TS_{E\rightarrow Z(\text{adiab})}$, Figure 2e) channel lies some ∼7 kcal mol^{-1} above $TS_{E\rightarrow Z(\text{nonadiab})}$.

Thus, the nonadiabatic *trans* → *cis* double-bond isomerization is predicted to be the process occuring in the experiments of Christensen et al. The existence of a "minimum → transition state → conical intersection" topology of the S_1 surface explains the abrupt increase in fluorescence decay rate[2,7] above 2100 cm^{-1} vibrational excess energy. The computed barrier (at $TS_{E\rightarrow Z(\text{nonadiab})}$) reproduces the observed fluorescence decay energy threshold within ∼1.5 kcal mol^{-1} (the 0−0 excitation energy is reproduced within ∼4 kcal mol^{-1} [9]. An analytical frequency computation at $TS_{E\rightarrow Z(\text{nonadiab})}$ yields a single imaginary frequency (73 *i* cm^{-1}). The lowest frequency *real* vibrational mode is 54 cm^{-1} which must be compared with the initial step (∼80 cm^{-1}) observed in the decay rate. There is no ambiguity in the assignment of the lowest frequency mode since the closest (computed) vibrations have frequencies of 126, 161, and 186 cm^{-1}.

The complex molecular structure progression along the MEP passing through $TS_{E\rightarrow Z(\text{nonadiab})}$ and connecting the S_1 Min to the S_1/S_0 conical intersection structure (CI, Figure 2f) is shown in Figure 1 (the computed MEP energy profiles are given in the supporting information). The gradual formation of a "$-(CH)_3-$" kink (indicated by three filled carbon atoms in Figure 1) along the path to the intersection appears to be a general feature of the radiationless decay channel of linear polyenes and polyene radicals.[10] The ∼75° C_3-C_4 double-bond twist achieved at the intersection point suggests that the decay channel is associated with *trans* → *cis* isomerization motion.

In conclusion, we have found that, in the conditions of the cool jet experiment of refs 2 and 7, photoinduced adiabatic *trans* → *cis* isomerization of *all-trans*-OT will not occur. This result is in contrast with the isomerization mechanism proposed by Kohler on the basis of matrix isolation experiments.[3] However, in that case, dominance of an adiabatic *trans* → *cis* channel may be a consequence of the constrained motion in the matrix cavity. As illustrated in Figure 1, our computations support the hypothesis that the nonadiabatic *trans* → *cis* motion initiated on S_1 and prompting the opening of the observed decay channel will be completed on the ground state. This must be the major photochemical channel in *all-trans*-OT since the spectroscopic S_2 (1Bu) state undergoes very rapid radiationless decay to the S_1 state.[11] Christensen, Yoshihara, and Petek et al.[7] have related the 80 cm^{-1} step in the S_1 decay rate to the in-plane bending motion of the reactant. However, due to the exceptionally different geometry of the reactant and the transition state (see Figure 2e,a), their vibrational modes are expected to be almost unrelated. Indeed our results indicate that the step feature is due to the (53 cm^{-1}) mode (represented in Figure 1) which corresponds to an allyl fragment twisting.

Acknowledgment. This research has been supported in part by the EPSRC (U.K.) under grant number GR/H94177. We are also grateful to NATO for the grant no. CRG 950748.

Supporting Information Available: One figure (Figure 3) containing the S_1 and S_0 MCSCF energy profiles along the S_1 MEP describing the *trans* → *cis* path from *all-trans*-OT toward the S_1/S_0 crossing point and the cartesian coordinates of all structures discussed in the text (7 pages). See any current masthead page for ordering and Internet access instructions.

JA961707H

(9) A more accurate multireference−MP2 computation of the O−O excitation energy of *all-trans*-OT has been reported by Roos et al. (Serrano-Andrés, L.; Lindh, R.; Roos, B. O.; Merchán, M. *J. Phys. Chem.* **1993**, *97*, 9360−9368). Since it is known that adiabatic barriers on covalent states are less sensitive to basis set and active space expansion, we have used a less demanding level of theory.

(10) Celani, P.; Garavelli, M.; Ottani, S.; Bernardi, F.; Robb, M. A.; Olivucci, M. *J. Am. Chem. Soc.* **1995**, *117*, 11584−11585.

(11) Shreve, A. P.; Trautman, J. K.; Owens, T. G.; Albrecht, A. C. *Chem. Phys. Lett.* **1991**, *89*, 178. The $S_2 \rightarrow S_1$ fast radiationless decay is probably due to the presence of a conical intersection. See: (a) Vaida, V. *Acc. Chem. Res.* **1986**, *114*, 19. (b) Petek, H.; Bell, A. J.; Yoshihara, K.; Christensen *J. Chem. Phys.* **1991**, *95*, 4739.